GEOLOGY | THE GEOLOGICAL SOCIETY OF AMERICA®

https://doi.org/10.1130/G52457.1

Manuscript received 8 June 2024
Revised manuscript received 16 August 2024
Manuscript accepted 25 August 2024

Published online 10 September 2024

The timing and duration of large-scale carbon release in the Early Jurassic

David B. Kemp[1,*], Jahandar Ramezani[2], Kentaro Izumi[3], Aisha Al-Suwaidi[4], Chunju Huang[1], Wenhan Chen[5,6], and Yuqing Zhu[1]

[1]State Key Laboratory of Biogeology and Environmental Geology and Hubei Key Laboratory of Critical Zone Evolution, School of Earth Sciences, China University of Geosciences, Wuhan 430074, P.R. China
[2]Department of Earth, Atmospheric and Planetary Sciences, Massachusetts Institute of Technology, Cambridge, Massachusetts 02139, USA
[3]Faculty & Graduate School of Education, Chiba University, 1-33 Yayoi-cho, Inage-ku, Chiba-shi, Chiba 263-8522, Japan
[4]Department of Earth Sciences, Khalifa University of Science and Technology, P.O. Box 127788, 28 Abu Dhabi, UAE
[5]State Key Laboratory of Oil and Gas Reservoir Geology and Exploitation and Institute of Sedimentary Geology, Chengdu University of Technology, Chengdu 610059, P.R. China
[6]International Center for Sedimentary Geochemistry and Biogeochemistry Research, Chengdu University of Technology, Chengdu 610059, P.R. China

ABSTRACT

The Toarcian oceanic anoxic event (T-OAE, ca. 183 Ma) in the Early Jurassic was one of the most significant warming events of the Phanerozoic, associated with large-scale carbon emissions, mass extinction, and perturbations to hydrology and ocean chemistry. However, the age and duration of this hyperthermal have long been uncertain, hindering our understanding of the timing and pace of carbon release and the associated environmental and biotic changes. We present high-precision radioisotopic dates bracketing a biostratigraphically constrained record of the T-OAE in Japan. Our geochronology reveals an unexpectedly short T-OAE duration of ~300 k.y. and a temporal coincidence with Ferrar large igneous province (LIP) magmatism. Our dates refute previous work linking the T-OAE to the earlier Karoo LIP, which was coincident with an earlier carbon cycle perturbation at the Pliensbachian–Toarcian boundary. Our results suggest both events were driven by extremely rapid (perhaps sub-millennial scale) thermogenic carbon degassing during LIP sill intrusion.

INTRODUCTION

The Toarcian oceanic anoxic event (T-OAE, or Jenkyns event, ca. 183 Ma) in the Early Jurassic was one of the most significant hyperthermal events of the Phanerozoic. It was characterized by seawater warming of up to 5 °C (Bailey et al., 2003), widespread ocean deoxygenation (e.g., Kemp et al., 2022), increased chemical weathering and hydrological cycling (Izumi et al., 2018; Kemp et al., 2020), and extinction (e.g., Danise et al., 2015). The event is recognized in the sedimentary record by a negative carbon-isotope excursion (CIE) affecting biospheric reservoirs of carbon (e.g., Hesselbo et al., 2000; Izumi et al., 2012; Them et al., 2017). The CIE implies the release of a large mass of ^{12}C-enriched carbon to the ocean-atmosphere system, a deduction that is supported by proxy data evidence for a likely doubling of atmospheric CO_2 (Ruebsam et al., 2020). The source of this carbon is debated, but a broad temporal overlap between the T-OAE and magmatism in the Karoo and/or Ferrar large igneous provinces (LIPs; southern Africa and Antarctica) has led to suggestions that volcanic CO_2 degassing and/or thermogenic carbon release from sill intrusion into organic-rich rocks provided the bulk of the carbon (McElwain et al., 2005; Svensen et al., 2007, 2012). A link to magmatism is also supported by mercury (Hg) enrichment that occurs coevally with the CIE in some sedimentary records of the event (e.g., Percival et al., 2015). An alternative hypothesis is that carbon was sourced largely from biogenic sources, such as marine methane hydrates, permafrost, and/or soils (e.g., Hesselbo et al., 2000; Kemp et al., 2005; Them et al., 2017).

A longstanding limitation to our understanding of the T-OAE has been the lack of a robust age and time scale for the event. This knowledge gap hinders a full understanding of both the timing of the event in relation to the hypothesized Karoo and/or Ferrar LIP driver and the pace and duration of carbon release and associated paleoenvironmental and biotic changes. The CIE has been proposed to span anywhere from 300 k.y. to 1.5 m.y. (e.g., Hesselbo et al., 2000; Huang and Hesselbo, 2014; Boulila et al., 2014; Ikeda et al., 2018; Thibault et al., 2018; Ruebsam and Al-Husseini, 2020), with these previous estimates largely reliant on cyclostratigraphy. In recent years, most studies have accepted a long (>1 m.y.) duration for the event (see esp. Hesselbo et al., 2020). This view is contested, however (Kemp et al., 2005; Boulila et al., 2014; Sell et al., 2014; Ikeda et al., 2018), and the debate has hitherto remained unresolved owing to an absence of high-precision radioisotopic dates in sections with unambiguous expression of the CIE.

Our study addressed the longstanding T-OAE chronology debate and determined the age and duration of the T-OAE using high-precision zircon U-Pb geochronology obtained from volcanic tuffs exposed in Japan that bracket the CIE in an expanded, chemo- and biostratigraphically constrained sedimentary record of the event.

David B. Kemp https://orcid.org/0000-0002-5116-5046
*davidkemp@cug.edu.cn

CITATION: Kemp, D.B., et al., 2024, The timing and duration of large-scale carbon release in the Early Jurassic: Geology, v. 52, p. 891–895, https://doi.org/10.1130/G52457.1

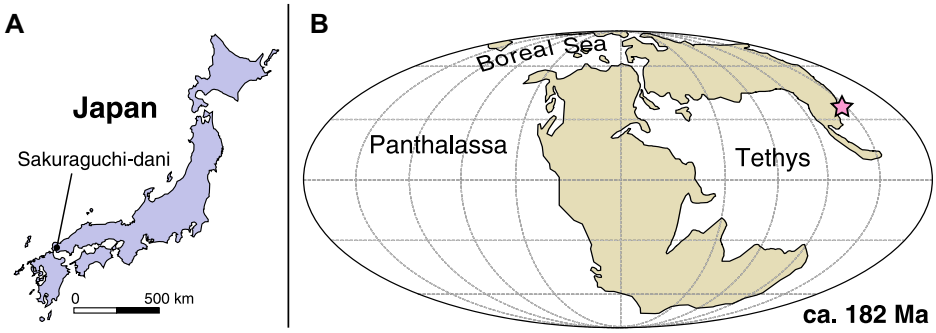

Figure 1. Maps showing the modern location (A; 34°08′N, 131°03′E) and paleogeographic position (B; ca. 182 Ma) of the Sakuraguchi-dani section in Japan (pink star). Modified from Izumi et al. (2012).

MATERIALS AND METHODS

The Sakuraguchi-dani section in the Tabe Basin of Japan (34°08′N, 131°03′E; Fig. 1) was deposited on the margin of the Panthalassa Ocean and preserves an ~90-m-thick record of lower Toarcian shallow marine siltstones, mudstones, and sandstones (Fig. 2). A detailed ammonite biostratigraphy (Nakada and Matsuoka, 2011; Izumi et al., 2012), coupled with organic carbon isotope ($\delta^{13}C_{org}$) data (Izumi et al., 2012, 2018; Kemp and Izumi, 2014; Kemp et al., 2020), confirms the presence of the T-OAE CIE, which spans 45.26 m of strata (–12.36 m to 32.9 m section height; Fig. 2; see also Text S1 in the Supplemental Material[1] for details of CIE definition).

We analyzed zircon grains from three volcanic tuff horizons in the section using the

[1]Supplemental Material. Texts S1–S3 (full description of methods and details of the Sakuraguchi-dani section), Figures S1–S3, and Table S1. Please visit https://doi.org/10.1130/GEOL.S.26858029 to access the supplemental material; contact editing@geosociety.org with any questions.

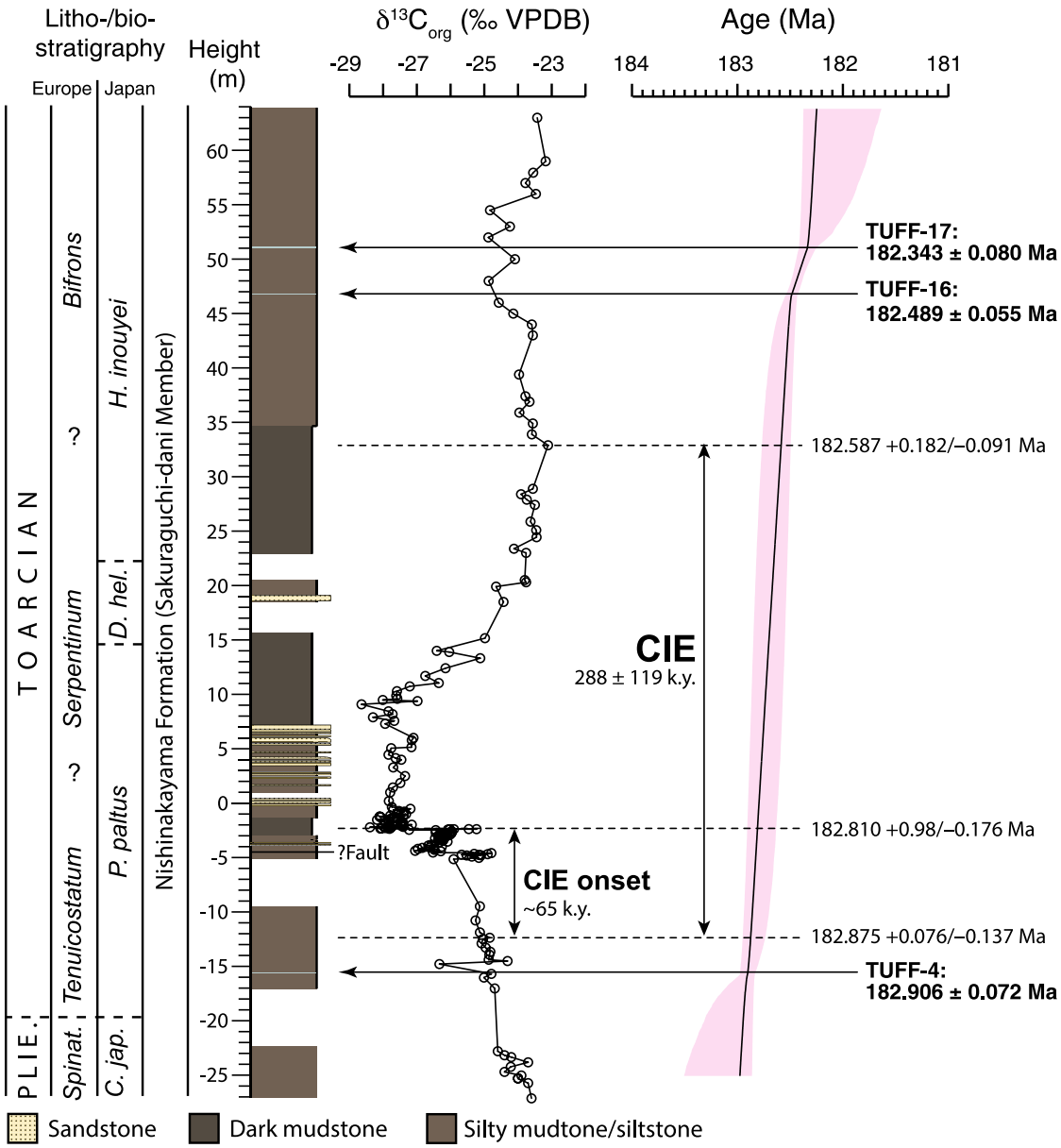

Figure 2. Lithostratigraphy, biostratigraphy, organic carbon isotope ($\delta^{13}C_{org}$) record, and chemical abrasion–isotope dilution–thermal ionization mass spectrometry (CA-ID-TIMS) U-Pb geochronology from Sakuraguchi-dani (Japan). Lithostratigraphy and $\delta^{13}C_{org}$ data are from Kemp et al. (2020). Ammonite biostratigraphy and correlation to northwest European ammonite provinces is based on Nakada and Matsuoka (2011) and Kemp and Izumi (2014) (see Text S2 [see footnote 1] for full details). Bayesian age-stratigraphic model results are also shown (BChron, Haslett and Parnell, 2008; Text S1), with ages and durations of key intervals marked. Pink shading is the 95% confidence interval. CIE—Toarcian oceanic anoxic event carbon isotope excursion; PLIE.—Pliensbachian; VPDB—Vienna Peedee belemnite. Ammonite zones: *Spinat.—Spinatum*; *C. jap.—Canavaria japonica*; *P. paltus—Protogrammoceras* (*Paltarpites*) *paltus*; *D. hel.—Dactylioceras helianthoides*; *H. inouyei—Harpoceras inouyei.*

TABLE 1. SUMMARY OF CALCULATED SAKURAGUCHI-DANI (JAPAN) U-Pb AGES AND THEIR UNCERTAINTIES

Sample	Stratigraphic height* (m)	$^{206}Pb/^{238}U$ age (Ma)	Uncertainty (2σ)†			MSWD§	*n*#	Total number of analyses
			X	*Y*	*Z*			
TUFF-17	51.07	182.343	0.080	0.11	0.23	0.93	3	5
TUFF-16	46.83	182.489	0.055	0.099	0.22	1.3	5	6
TUFF-4	–15.58	182.906	0.072	0.11	0.22	1.2	4	5

Note: Full data set is provided in Table S1 (see text footnote 1).
*Stratigraphic elevation is relative to first major sandstone bed in the section (0 m datum, see Fig. 2).
†*X*—internal (analytical) uncertainty in the absence of all external or systematic errors; *Y*—incorporates the U-Pb tracer calibration error; *Z*—includes *X* and *Y*, as well as the uranium decay constant errors of Jaffey et al. (1971).
§MSWD—mean square of weighted deviates.
#*n* is the number of analyses included in the calculated weighted mean date out of the total number of analyses.

high-precision chemical abrasion–isotope dilution–thermal ionization mass spectrometry (CA-ID-TIMS) U-Pb method (see Text S1 for full details). The lowest of these tuff horizons (TUFF-4, –15.58 m) is below the CIE and biostratigraphically constrained to the *Protogrammoceras (Paltarpites) paltus* ammonite, equivalent to the *Tenuicostatum* Zone in northwest Europe (Nakada and Matsuoka, 2011; Fig. 2, Text S2). The upper two tuff horizons (TUFF-16 and TUFF-17 at 46.83 m and 51.07 m, respectively) are above the CIE and biostratigraphically constrained to the *Harpoceras inouyei* Zone, likely equivalent to the *Bifrons* Zone in northwest Europe (Nakada and Matsuoka, 2011; Fig. 2, Text S2).

RESULTS

Our analyses yielded weighted mean $^{206}Pb/^{238}U$ ages of 182.906 ± 0.072 Ma for TUFF-4 (–15.58 m), 182.489 ± 0.055 Ma for TUFF-16 (46.83 m), and 182.343 ± 0.080 Ma for TUFF-17 (51.07 m) (Table 1; Fig. 2; Fig. S1). The two dated tuffs that bracket the CIE (TUFF-4 and TUFF-16) define a duration for the intervening 62.41 m of strata of 0.417 ± 0.091 m.y. Bayesian age-stratigraphic modeling (BChron, Haslett and Parnell, 2008; Text S1) yields a duration of 0.288 ± 0.119 m.y. for the 45.26 m CIE itself, and an age of 182.875 +0.076/–0.137 Ma for the CIE onset at –12.36 m (Figs. 2 and 3).

DISCUSSION AND CONCLUSIONS

The Timing and Duration of Carbon Release at the T-OAE

Our high-precision geochronology and Bayesian age model demonstrate that the

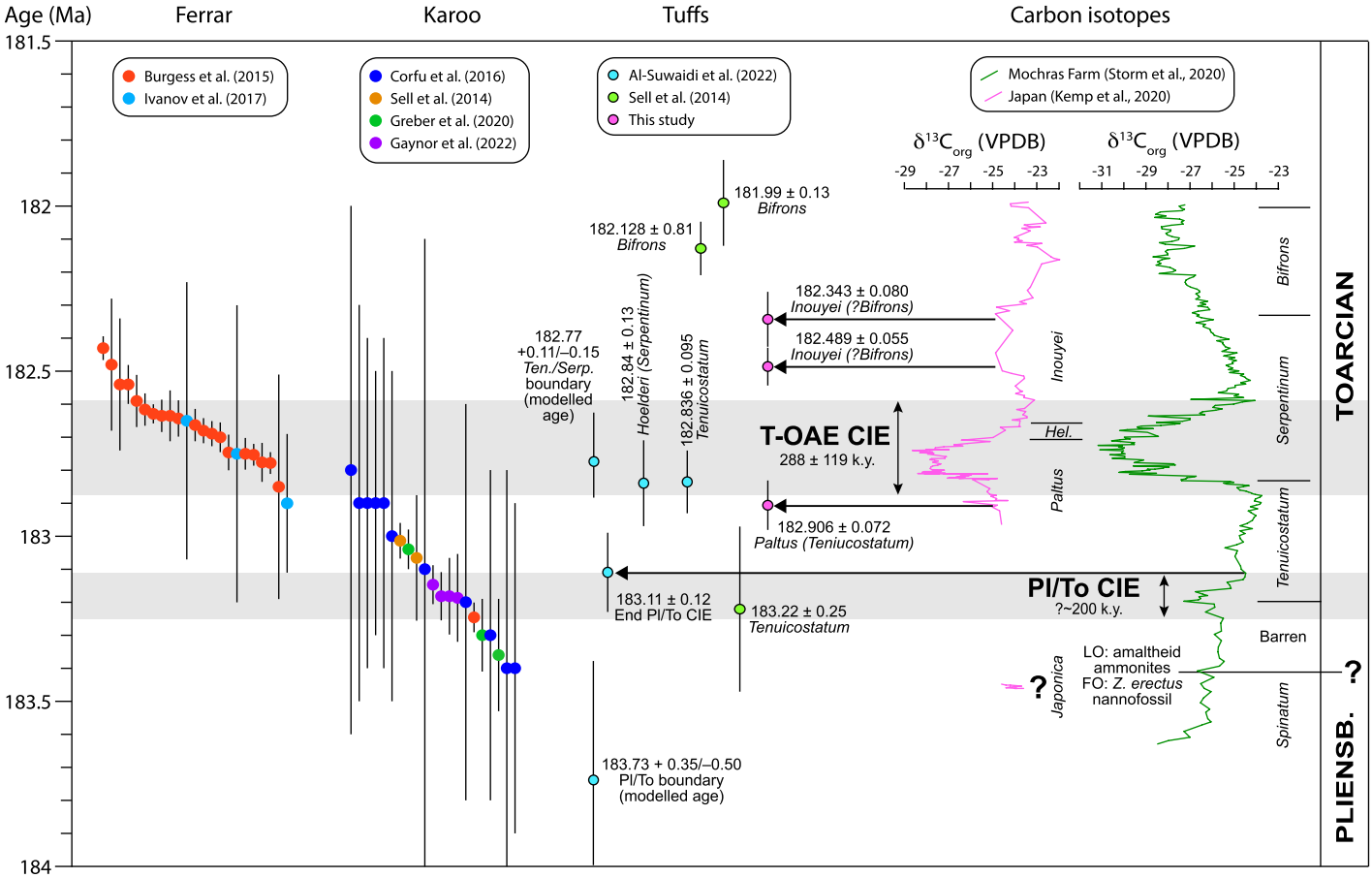

Figure 3. Compilation of modern U-Pb geochronologic data for Karoo and Ferrar large igneous province magmatism and for interbedded tuffs through the late Pliensbachian (PLIENSB.) and early Toarcian. Age data are plotted against the $\delta^{13}C_{org}$ data of Sakuraguchi-dani, Japan (Fig. 2), and the reference section of the Mochras Farm (Llanbedr) borehole in Wales (UK) (Storm et al., 2020). Note the temporal coincidence of the negative carbon isotope excursion (CIE) at the Pliensbachian–Toarcian boundary (Pl/To) and the Toarcian oceanic anoxic event (T-OAE) with Karoo and Ferrar magmatism, respectively. The Sakuraguchi-dani $\delta^{13}C_{org}$ record is converted to time using our U-Pb geochronology and a Bayesian (BChron, Haslett and Parnell, 2008) age-stratigraphic model, with a hiatus inferred between the *Protogrammeroceras* (*Paltarpites*) *paltus* and *Canavaria japonica* ammonite zones (see Text S2 [see text footnote 1]; *C. japonica* Zone data are marked with a question mark to highlight numerical age uncertainty). Mochras Farm $\delta^{13}C_{org}$ data are converted to time by anchoring the start and end of the T-OAE CIE to our modeled ages of 182.875 Ma and 182.587 Ma, respectively, and the end of the Pl/To CIE to 183.11 Ma (Al-Suwaidi et al., 2022). Linear interpolation is used to scale the rest of the data, except below the Pl/To CIE where $\delta^{13}C_{org}$ ages are based on the cyclostratigraphy of Storm et al. (2020). The possible Pliensbachian–Toarcian boundary position at Mochras Farm is from Bodin et al. (2023). VPDB—Vienna Peedee belemnite; *Hel.—helianthoides*; FO—first occurrence; LO—last occurrence; *Z. erectus—Zeugrhabdotus erectus*.

T-OAE CIE spanned a minimum of 169 k.y., and was likely no longer than 407 k.y., taking in account the propagated uncertainties of the age model. The geochronology, and in particular this maximum likely duration, is robust to possible changes in sedimentation rate in the succession caused by the presence of rapidly deposited sandstone event beds in the CIE (Text S3; Fig. S2; Izumi et al., 2018).

Our findings refute suggestions that the CIE lasted ~1 m.y. or longer (e.g., Thibault et al., 2018; Hesselbo et al., 2020; Ruebsam and Al-Husseini, 2020), which are based mainly on cyclostratigraphy and, in particular, the deduction that cycles in $\delta^{13}C$ through the CIE onset were controlled by ~100 k.y. orbital eccentricity (Hesselbo et al., 2020, and references therein). By contrast, our duration matches well with previous estimates of ~300–500 k.y. from multiple sections based on the assignment of the $\delta^{13}C$ onset cycles to 35 k.y. orbital obliquity (e.g., Boulila et al., 2014). Equally, both the ages and duration that we define agree with an astronomically calibrated chronology from a deep-water chert sequence (Ikeda et al., 2018), which calibrated the age span of the T-OAE CIE (as expressed by a –5‰ excursion in $\delta^{13}C_{org}$) as 182.9 ± 0.2 Ma to 182.6 ± 0.2 Ma. A <407 k.y. duration for the event is also consistent with existing, but less precise, radioisotopic age constraints based on minimum error interpolation of zircon U-Pb dates obtained from below and well above the assumed interval of the T-OAE in Peru (Sell et al., 2014; Fig. 3; Fig. S3). In that Peru section, the CIE is unclear, but the geochronology, as well as recent high-precision U-Pb data from the *Tenuicostatum* Zone (Al-Suwaidi et al., 2022; Fig. 3; Fig. S3), provide strong support that the CIE duration was significantly shorter than 1 m.y. (Fig. S3).

The T-OAE CIE, as recorded worldwide, comprises an onset interval (defined by the shift to minimum $\delta^{13}C$ values; Fig. 2) that demarcates the period over which ^{12}C-enriched carbon release to the biosphere is inferred to have occurred. This is typically followed (as is the case at Sakuraguchi-dani) by an interval of low but stable $\delta^{13}C$, and then a relatively protracted recovery back to near pre-event $\delta^{13}C$ values (Ruebsam and Al-Husseini, 2020, and references therein). Considering our Sakuraguchi-dani record specifically, our Bayesian age-stratigraphic model indicates that the CIE onset, and hence carbon release, occurred over ~65 k.y. (–12.36 m to –2.21 m; Fig. 2). Although a fault may have interrupted the onset interval (–4.58 m in Fig. 2) the proportion of the CIE encompassed by the onset interval is comparable with other globally distributed records (spanning ~30% of the total CIE thickness; Ruebsam and Al-Husseini, 2020), emphasizing the likelihood of an onset duration of <100 k.y. Moreover, even if an unrealistically large thickness of rock was missing from the CIE onset interval at Sakuraguchi-dani due to the possible fault, it would not significantly alter our calculated CIE duration (Text S3). Importantly, abrupt (centimeter-scale) decreases in $\delta^{13}C$ during the CIE onset are recognized in sections sampled at high resolution globally, including at Sakuraguchi-dani (e.g., Kemp et al., 2005; Them et al., 2017; Izumi et al., 2018; Ruebsam and Al-Husseini, 2020; Fig. 2). Although the time scales of these abrupt shifts are subject to significant error given their stratigraphic brevity (and because it is possible that hiatuses altered their abruptness and morphology), these likely correlatable shifts (e.g., Izumi et al., 2018) imply that the bulk of ^{12}C-enriched carbon was released in discrete pulses occurring on millennial, or possibly shorter, time scales (a possibility previously suggested by Kemp et al., 2005, 2020, and Them et al., 2017). In the case of the Sakuraguchi-dani CIE record, for instance, a sharp –2.9‰ negative $\delta^{13}C_{org}$ shift at –2.38 m spans just 5 cm (Izumi et al., 2018; Fig. 2), implying carbon release over <1000 yr based on our CIE duration and Bayesian age model.

Synchronicity of Early Jurassic Carbon Release and Magmatism

Our modeled ages for the start and end of the CIE are synchronous (within error) with the timing and duration of sill emplacement and effusive volcanism in the Ferrar LIP (182.779 ± 0.033 Ma to 182.430 ± 0.036 Ma), as determined by CA-ID-TIMS U-Pb geochronology of comparable resolution (Burgess et al., 2015; Fig. 3). This coincidence strongly supports a causal link. The likely transience of sill emplacement in particular implies rapid magma fluxes through country rocks and potentially high levels of CO_2 and CH_4 generation from contact metamorphism of organic carbon–rich sedimentary rocks (Svensen et al., 2012). Explosive release of thermogenic carbon via this mechanism has been considered a key source of the carbon released at the T-OAE (Svensen et al., 2007, 2012), likely in concert with more protracted volcanic degassing (Heimdal et al., 2021). The pulsed, extremely rapid release of carbon we infer is fully consistent with this proposed mechanism. Indeed, this mechanism of thermogenic carbon release, including its likely rapidity, is also supported by carbon cycle modeling (Heimdal et al., 2021) and chemostratigraphic Hg data (Percival et al., 2015). Nevertheless, our data do not entirely preclude the involvement of other sources of carbon, including surficial biogenic sources that could have been liberated in a similarly rapid manner due to feedbacks initiated by T-OAE warming (e.g., Them et al., 2017; Ruebsam et al., 2020).

Previous studies have suggested that thermogenic and/or volcanic carbon release from the Karoo LIP was the driver of the T-OAE (Svensen et al., 2007, 2012; Greber et al., 2020; Heimdal et al., 2021; Gaynor et al., 2022), but these studies assumed an older age for the T-OAE than our data now indicate. Our new geochronology (and the U-Pb dating of Al-Suwaidi et al., 2022) does, however, demonstrate that Karoo magmatism was coeval with a distinctly earlier climate perturbation and negative CIE at the Pliensbachian–Toarcian boundary (Pl/To event) that had a similarly short duration of ~200 k.y. (Al-Suwaidi et al., 2022, and references therein; Fig. 3). Specifically, a high-precision U-Pb date (183.11 ± 0.12 Ma) from Argentina that marks the end of the Pl/To CIE (Al-Suwaidi et al., 2022) indicates that this CIE was synchronous with rapid basin-wide sill emplacement associated with the Karoo LIP, which has been constrained recently to between 183.187 ± 0.133 Ma and 183.147 ± 0.059 Ma (Gaynor et al., 2022; Fig. 3). As such, the Pl/To and T-OAE events likely had similar causes, but were temporally distinct. Moreover, the cause of both events appears to have been similar to the younger Paleocene–Eocene Thermal Maximum (PETM) hyperthermal (ca. 56 Ma, duration of ~200 k.y.), where clear evidence for rapid and explosive venting of thermogenic carbon has now been obtained from seismic imaging and borehole records from the Norwegian margin of the contemporaneous North Atlantic LIP (Berndt et al., 2023).

Our determination of the age and time scale for the T-OAE underlines the transience of this major hyperthermal event, and provides a robust framework for understanding the pace and duration of the many environmental and biotic changes that were associated with it. Our work also strongly supports the emerging view that geologically rapid thermogenic carbon release related to sill emplacement was a primary driver of large-scale climate change in Earth's history.

ACKNOWLEDGMENTS

This work was supported by the National Key R&D Program of China (grant 2023YFF0804000), the National Natural Science Foundation of China (grants 42230208, 41888101), and the Natural Environment Research Council of the UK (grant NE/I02089X/1). K. Izumi acknowledges support from the Japan Society for the Promotion of Science (grants KAKENHI 12J08818 and 15J08821). This is a contribution to the International Geoscience Programme IGCP739. The authors thank Slah Boulila, Stéphane Bodin, and an anonymous reviewer for helpful comments on an earlier draft of this manuscript.

REFERENCES CITED

Al-Suwaidi, A.H., et al., 2022, New age constraints on the Lower Jurassic Pliensbachian–Toarcian Boundary at Chacay Melehue (Neuquén Basin, Argentina): Scientific Reports, v. 12, 4975, https://doi.org/10.1038/s41598-022-07886-x.

Bailey, T.R., Rosenthal, Y., McArthur, J.M., van de Schootbrugge, B., and Thirlwall, M.F., 2003, Paleoceanographic changes of the Late Pliensbachian–Early Toarcian interval: A possible link to the genesis of an Oceanic Anoxic Event:

Earth and Planetary Science Letters, v. 212, p. 307–320, https://doi.org/10.1016/S0012-821X(03)00278-4.

Berndt, C., et al., 2023, Shallow-water hydrothermal venting linked to the Paleocene Eocene Thermal Maximum: Nature Geoscience, v. 16, p. 803–809, https://doi.org/10.1038/s41561-023-01246-8.

Bodin, S., Fantasia, A., Krencker, F.-N., Nebsbjerg, B., Christiansen, L., and Andrieu, S., 2023, More gaps than record! A new look at the Pliensbachian/Toarcian boundary event guided by coupled chemo-sequence stratigraphy: Palaeogeography, Palaeoclimatology, Palaeoecology, v. 610, https://doi.org/10.1016/j.palaeo.2022.111344.

Boulila, S., Galburn, B., Huret, E., Hinnov, L., Rouget, I., Gardin, S., and Bartolini, A., 2014, Astronomical calibration of the Toarcian stage: Implications for sequence stratigraphy and duration of the early Toarcian OAE: Earth and Planetary Science Letters, v. 386, p. 98–111, https://doi.org/10.1016/j.epsl.2013.10.047; corrigendum available at https://doi.org/10.1016/j.epsl.2014.09.036.

Burgess, S.D., Bowring, S.A., Fleming, T.H., and Elliot, D.H., 2015, High-precision geochronology links the Ferrar large igneous province with early-Jurassic ocean anoxia and biotic crisis: Earth and Planetary Science Letters, v. 415, p. 90–99, https://doi.org/10.1016/j.epsl.2015.01.037.

Corfu, F., Svensen, H.H., and Mazzini, A., 2016, Comment to paper: Evaluating the temporal link between the Karoo LIP and climatic–biologic events of the Toarcian Stage with high-precision U–Pb geochronology: Earth and Planetary Science Letters, v. 434, p. 349–352, https://doi.org/10.1016/j.epsl.2015.07.010.

Danise, S., Twitchett, R.J., and Little, C.T.S., 2015, Environmental controls on Jurassic marine ecosystems during global warming: Geology, v. 43, p. 263–266, https://doi.org/10.1130/G36390.1.

Gaynor, S.P., Svensen, H.H., Polteau, S., and Schaltegger, U., 2022, Local melt contamination and global climate impact: Dating the emplacement of Karoo LIP sills into organic-rich shale: Earth and Planetary Science Letters, v. 579, https://doi.org/10.1016/j.epsl.2022.117371.

Greber, N.D., Davies, J.H.F.L., Gaynor, S.P., Jourdan, F., Betrand, H., and Schaltegger, U., 2020, New high precision U-Pb ages and Hf isotope data from the Karoo large igneous province; Implications for pulsed magmatism and early Toarcian environmental perturbations: Results in Geochemistry, v. 1, https://doi.org/10.1016/j.ringeo.2020.100005.

Haslett, J., and Parnell, A., 2008, A simple monotone process with application to radiocarbon-dated depth chronologies: Journal of the Royal Statistical Society: Series C, Applied Statistics, v. 57, p. 399–418, https://doi.org/10.1111/j.1467-9876.2008.00623.x.

Heimdal, T.H., Goddéris, Y., Jones, M.T., and Svensen, H.H., 2021, Assessing the importance of thermogenic degassing from the Karoo Large Igneous Province (LIP) in driving Toarcian carbon cycle perturbations: Nature Communications, v. 12, 6221, https://doi.org/10.1038/s41467-021-26467-6.

Hesselbo, S.P., Gröcke, D.R., Jenkyns, H.C., Bjerrum, C.J., Farrimond, P., Morgans Bell, H.S., and Green, O.R., 2000, Massive dissociation of gas hydrate during a Jurassic oceanic event: Nature, v. 406, p. 392–395, https://doi.org/10.1038/35019044.

Hesselbo, S.P., Ogg, J.G., and Ruhl, M., 2020, The Jurassic Period, *in* Gradstein, F.M., et al., eds., Geologic Time Scale 2020: Amsterdam, Elsevier, p. 955–1021, https://doi.org/10.1016/B978-0-12-824360-2.00026-7.

Huang, C., and Hesselbo, S.P., 2014, Pacing of the Toarcian Oceanic Anoxic Event (Early Jurassic) from astronomical correlation of marine sections: Gondwana Research, v. 25, p. 1348–1356, https://doi.org/10.1016/j.gr.2013.06.023.

Ikeda, M., Hori, R.S., Ikehara, M., Miyashita, R., Chino, M., and Yamada, K., 2018, Carbon cycle dynamics linked with Karoo-Ferrar volcanism and astronomical cycles during Pliensbachian-Toarcian (Early Jurassic): Global and Planetary Change, v. 170, p. 163–171, https://doi.org/10.1016/j.gloplacha.2018.08.012.

Ivanov, A.V., Meffre, S., Thompson, J., Corfu, F., Kamenetsky, V.S., Kamenetsky, M.B., and Demonterova, E.I., 2017, Timing and genesis of the Karoo-Ferrar large igneous province: New high precision U-Pb data for Tasmania confirm short duration of the major magmatic pulse: Chemical Geology, v. 455, p. 32–43, https://doi.org/10.1016/j.chemgeo.2016.10.008.

Izumi, K., Miyaji, T., and Tanabe, K., 2012, Early Toarcian (Early Jurassic) oceanic anoxic event recorded in the shelf deposits in the northwestern Panthalassa: Evidence from the Nishinakayama Formation in the Toyora area, west Japan: Palaeogeography, Palaeoclimatology, Palaeoecology, v. 315–316, p. 100–108, https://doi.org/10.1016/j.palaeo.2011.11.016.

Izumi, K., Kemp, D.B., Itamiya, S., and Inui, M., 2018, Sedimentary evidence for enhanced hydrological cycling in response to rapid carbon release during the early Toarcian oceanic anoxic event: Earth and Planetary Science Letters, v. 481, p. 162–170, https://doi.org/10.1016/j.epsl.2017.10.030.

Jaffey, H., Flynn, K.F., Glendenin, L.E., Bentley, W.C., and Essling, A.M., 1971, Precision measurement of half-lives and specific activities of ^{235}U and ^{238}U: Physical Review C, v. 4, p. 1889–1906, https://doi.org/10.1103/PhysRevC.4.1889.

Kemp, D.B., and Izumi, K., 2014, Multiproxy geochemical analysis of a Panthalassic margin record of the early Toarcian oceanic anoxic event (Toyora area, Japan): Palaeogeography, Palaeoclimatology, Palaeoecology, v. 414, p. 332–341, https://doi.org/10.1016/j.palaeo.2014.09.019.

Kemp, D.B., Coe, A.L., Cohen, A.S., and Schwark, L., 2005, Astronomical pacing of methane release in the Early Jurassic period: Nature, v. 437, p. 396–399, https://doi.org/10.1038/nature04037; erratum available at https://doi.org/10.1038/nature04361.

Kemp, D.B., Selby, D., and Izumi, K., 2020, Direct coupling between carbon release and weathering during the Toarcian oceanic anoxic event: Geology, v. 48, p. 976–980, https://doi.org/10.1130/G47509.1.

Kemp, D.B., Suan, G., Fantasia, A., Jin, S., and Chen, W., 2022, Global organic carbon burial during the Toarcian oceanic anoxic event: Patterns and controls: Earth-Science Reviews, v. 231, https://doi.org/10.1016/j.earscirev.2022.104086.

McElwain, J.C., Wade-Murphy, J., and Hesselbo, S.P., 2005, Changes in carbon dioxide during an oceanic anoxic event linked to intrusion into Gondwana coals: Nature, v. 435, p. 479–482, https://doi.org/10.1038/nature03618.

Nakada, K., and Matsuoka, A., 2011, International correlation of the Pliensbachian/Toarcian (Lower Jurassic) ammonoid biostratigraphy of the Nishinakayama Formation in the Toyora Group, southwest Japan: Newsletters on Stratigraphy, v. 44, p. 89–111, https://doi.org/10.1127/0078-0421/2011/0006.

Percival, L.M.E., Witt, M.L.I., Mather, T.A., Hermoso, M., Jenkyns, H.C., Hesselbo, S.P., Al-Suwaidi, A.H., Storm, M.S., Xu, W., and Ruhl, M., 2015, Globally enhanced mercury deposition during the end-Pliensbachian extinction and Toarcian OAE: A link to the Karoo–Ferrar Large Igneous Province: Earth and Planetary Science Letters, v. 428, p. 267–280, https://doi.org/10.1016/j.epsl.2015.06.064.

Ruebsam, W., and Al-Husseini, M., 2020, Calibrating the early Toarcian (Early Jurassic) with stratigraphic black holes (SBH): Gondwana Research, v. 82, p. 317–336, https://doi.org/10.1016/j.gr.2020.01.011.

Ruebsam, W., Reolid, M., and Schwark, L., 2020, δ^{13}C of terrestrial vegetation records Toarcian CO_2 and climate gradients: Scientific Reports, v. 10, 117, https://doi.org/10.1038/s41598-019-56710-6.

Sell, B., Ovtcharova, M., Guex, J., Bartolini, A., Jourdan, F., Spangenberg, J.E., Vicente, J.-C., and Schaltegger, U., 2014, Evaluating the temporal link between the Karoo LIP and climatic–biologic events of the Toarcian Stage with high-precision U-Pb geochronology: Earth and Planetary Science Letters, v. 408, p. 48–56, https://doi.org/10.1016/j.epsl.2014.10.008.

Storm, M.S., Hesselbo, S.P., Jenkyns, H.C., Ruhl, M., Ullmann, C.V., Xu, W., Leng, M.J., Riding, J.B., and Gorbanenko, O., 2020, Orbital pacing and secular evolution of the Early Jurassic carbon cycle: Proceedings of the National Academy of Sciences of the United States of America, v. 117, p. 3974–3982, https://doi.org/10.1073/pnas.1912094117.

Svensen, H., Planke, S., Chevallier, L., Malthe-Sørenssen, A., Corfu, F., and Jamtveit, B., 2007, Hydrothermal venting of greenhouse gases triggering Early Jurassic global warming: Earth and Planetary Science Letters, v. 256, p. 554–566, https://doi.org/10.1016/j.epsl.2007.02.013.

Svensen, H., Corfu, F., Polteau, S., Hammer, Ø., and Planke, S., 2012, Rapid magma emplacement in the Karoo Large Igneous Province: Earth and Planetary Science Letters, v. 325–326, p. 1–9, https://doi.org/10.1016/j.epsl.2012.01.015.

Them, T.R., II, Gill, B.C., Caruthers, A.H., Gröcke, D.R., Tulsky, E.T., Martindale, R.C., Poulton, T.P., and Smith, P.L., 2017, High-resolution carbon isotope records of the Toarcian Oceanic Anoxic Event (Early Jurassic) from North America and implications for the global drivers of the Toarcian carbon cycle: Earth and Planetary Science Letters, v. 459, p. 118–126, https://doi.org/10.1016/j.epsl.2016.11.021.

Thibault, N., Ruhl, M., Ullmann, C.V., Korte, C., Kemp, D.B., Gröcke, D.R., and Hesselbo, S.P., 2018, The wider context of the Lower Jurassic Toarcian oceanic anoxic event in Yorkshire coastal outcrops, UK: Proceedings of the Geologists' Association, v. 129, p. 372–391.

Printed in the USA